Layered Pentahedral Mesh Generation for Biomechanical Geometries with Unclosed Surfaces

Zhipeng Lei and Jingzhou (James) Yang

Human-Centric Design Research Laboratory
Texas Tech University, Lubbock, TX 79409
Email: james.yang@ttu.edu

ABSTRACT

Available methods for automatic volumetric mesh generation require the inputted surface to be watertight. However, biomechanical geometries obtained from a 3D scanner, computed tomography (CT), or magnetic resonance (MRI) may not provide a closed surface. This paper proposes a layered pentahedral mesh generation method for a biomechanical geometry that is defined by any unclosed surface. Based on the initial geometries, two basic meshing problems for biomechanical model were solved. One is that the biomechanical geometry is defined by two surfaces and the volume bounded by the two surfaces is meshed. The other one is that the geometry defined by one surface and a list of points is meshed where there are predefined depths on these points. A distance function was defined for determining relative distance between a surface and a plane. The volumetric mesh was created by adding layers of pentahedral elements, and these pendtahedral elements were smoothed using the signal processing method. The proposed method was demonstrated with examples of meshing the deadspace of headform/respirator and developing the finite element model of a human face with different soft tissue thicknesses. Further, two applications, the CFD simulation of air leakage of headform/respirator and finite element contact simulation between a headform and a respirator, used the proposed method to create volumetric mesh. Results show that the proposed mesh method was able to create biomechanical models with acceptable mesh qualities from highly curved geometries.

Keywords: layered pentahedral mesh, respirator, biomechanical geometry.
DOI: 10.3722/cadaps.2013.231-245

1 INTRODUCTION

In 2003, NIOSH conducted an anthropometric survey of 3997 U.S. civilian workers and developed a new respirator fit test panel based on two principal components, which in turn are functions of 10 facial dimensions [25],[27]. Five representative headforms for the five size categories (large, medium, small, long/narrow and short/wide) were developed based on the data collected with traditional measurement tools and 3D data from a head scanner [26]. The complicated geometry of human headform causes troubles during the volumetric mesh to computational simulations that include the contact simulation between a headform and a respirator and the computational fluid dynamics (CFD) simulation of respirator/headform leakage [10],[11].

Deformable headform models have been adopted in the applications of facial expression and surgical simulations [11]. Facial animations used a layered mass spring model that is a simplified elastic model [13],[19]. Although a layered structure of facial model had the skin, muscle, and bone layers, they were modeled as triangular surfaces [9],[20]. Biomechanical applications prefer volumetric finite element models that can provide bio-fidelity and accuracy. However, the generation of volumetric mesh for human face is difficult. Barbarino et al. [2] constructed a 3D finite element model of human face that consisted of skin, fat, bones, muscles, and superficial system. Magnetic resonance images were used to generate hexahedron elements. This model is by far the most bio-fidelity facial model and has nonuniform layer thickness. However, the method for finite element mesh generation in the paper was explained very briefly and it is hard to be duplicated.

In several studies, the air flow around a headform or a whole human body has been simulated by the CFD method [1],[5]. These models did not contain the clothing, respirator, helmet, and glasses that are commonly used by typical wearers. An N95 respirator is made of permeable, nonwoven textiles (generally, polypropylene). Numerical simulations of virus diffusion through face masks and thermal interactions between the textiles and human skin were carried out without the incorporation of a 3D headform model [12],[14].

The octree-based method, advancing front method, and the Delaunay triangulation method are three most popular ways to generate unstructured volumetric mesh [4],[15],[20]. Among them, the octree-based method has been widely used in generating biomechanical models [8],[21-24]. While octree-based method contained a complex process of mesh refinement, Boyd and Müller [3] and Flaig [6] proposed a simplified octree-based method without mesh refinement. Instead, they used a signal processing method for mesh smoothing. This smoothing method was originally created by Taubin [16]. All these available mesh generation methods require the input data to be a watertight surface. However, biomechanical geometries are normally obtained by a 3D scanner, MRI or CT. Therefore, in the real world a closed surface does not exist.

This paper proposes an unstructured volume mesh generation method for a biomechanical geometry that is defined by any unclosed surfaces. Based on the initial geometries, two kinds of biomechanical model meshing problems are solved: (1) The biomechanical geometry is defined by two surfaces and the volume bounded by them is meshed; (2) the geometry defined by one surface and a list of points is meshed where on these points there are predefined depths. The rest of this paper is organized as follows: Section 2 presents the methodology. Sections 3 provides two specific applications, CFD simulation of air leakage of headform/respirator and the finite element contact between a headform and a respirator, in order to examine our proposed methods. Section 4 gives the conclusion and future work.

2 METHOD

Fig. 1 and 2 present the flowcharts for the problems of generating meshes of (1) a volume bounded by two individual surfaces and (2) a volume defined by a surface and a list of control points, respectively. Fig. 2 shows that the second problem will be transferred to the first problem to solve. We use the example of meshing headform/respirator's deadspace bounded by the human frontal face and the respirator to demonstrate the procedure of solving the first problem, including preprocessing two surfaces, determining distance functions, distributing nodes, generating pentahedrons and smoothing the volumetric mesh. We also use the example of generating a finite element human face model with predefined tissue thickness at different locations to demonstrate how to create a virtual surface from a list of control points and how to solve the second problem.

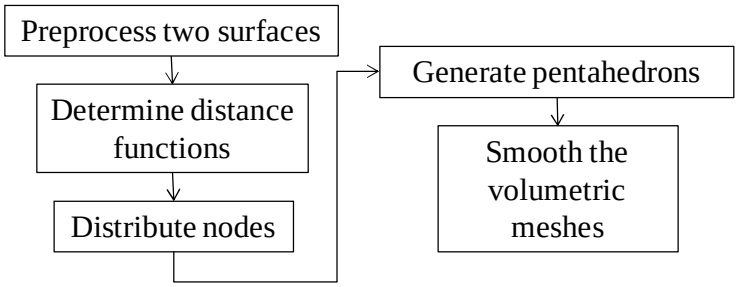

Fig.1: Flowchart of generating pentahedral mesh for a volume bounded by two surfaces.

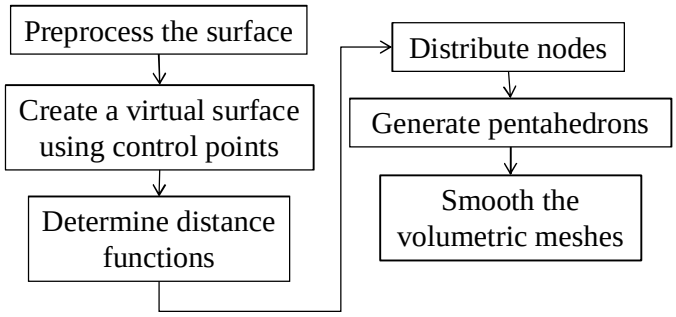

Fig. 2: Flowchart of generating pentahedral mesh for a volume defined by a surface and a list of control points.

2.1 Preprocessing

Computational methods have been used to study respirator fit and comfort [10],[11]. Respirator leakages were determined by simulating the air flow pattern inside the deadspace [10]. Consider a N95 filtering facepiece respirator (3M 8210) that is donned by a human headform (medium size). Their relative position after donning is calculated by a finite element contact simulation [11]. Fig. 3(a) denotes the inner surface of the respirator and the outer surface of the headform that are extracted from the final state of the contact simulation. The objective is to develop an algorithm to mesh the deadspace bounded by the surfaces of the human frontal face and the respirator for the CFD simulation of air flow inside the deadspace. Because a closed surface covering the deadspace is not available, commercial mesh software cannot be directly used.

The headform outer surface and the respirator inner surface are inputs in the form of polygons (or triangles). The geometries of these surfaces are mathematically described as vertices and triangles. Each vertex is denoted by a unique index and its global Cartesian coordinates, and each triangle is defined by the indices of three vertices. The respirator and headform surfaces are placed in the same global coordinate system, in which the z-coordinate is in the direction normal to the headform frontal face, the x-coordinate is along the lateral direction of the headform, and the y-coordinate is along the vertical direction of the headform. The origin of the global coordinate system is located on the intersection point of three perpendicular planes (the sagittal plane, coronal plane and transverse plane that pass through the nose tip point) and the x, y and z axes parallel to the intersection lines of these planes. Because only cheek, nose, chin, and neck areas of the headform interact with the respirator, the headform surface is trimmed for computational efficiency, as shown in Fig. 3(b).

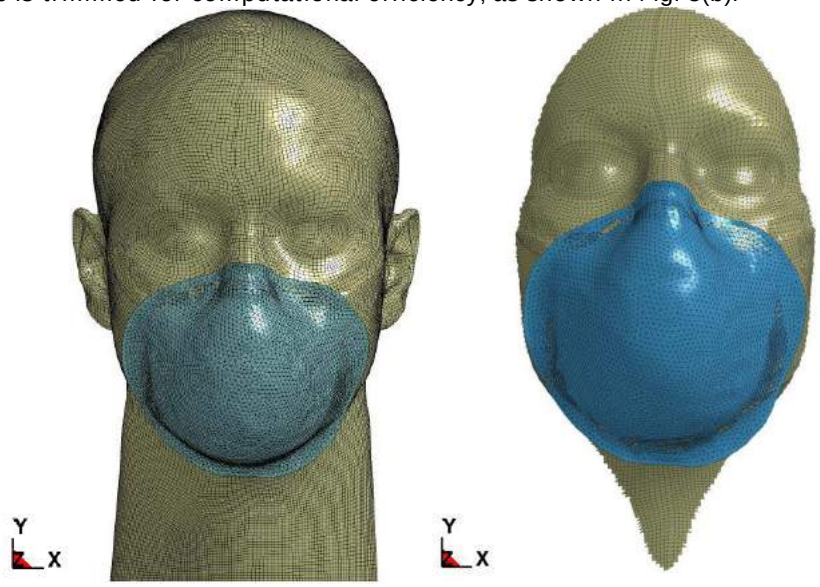

(a) (b)

Fig. 3: (a) The inner surface of the respirator and the outer surface of the headform; (b) the inner surface of the respirator and the trimmed surface of the headform.

2.2 Distance Functions

The kernel of the automatic mesh generation algorithm is based on geometry projections. The surfaces of the headform and the respirator are separately projected along the z axial direction to the xoy plane in order to obtain Segment K that contains the union of these two projection areas on the xoy plane. Segment K was discretized into nodes and rectangular grids and the grid sizes determine the element sizes of the volumetric mesh in the x and y axial direction. Then, by projecting every node of Segment K along the z axial direction to the headform and respirator surfaces and introducing the distance function $Dist(\mathbf{v}_i, S)$, where $\mathbf{v}_i$ was the position vector of Node i of the xoy plane and Surface S was either the respirator surface or the headform surface, we calculated the projecting distance between every node of Segment K and Surface S (either the respirator or headform surface).

The distance function for a surface and a node is defined for mathematically determining the geometrical relationship between the surface and the xoy plane. For any Node i ($i = 1,2,3,...,n$, where

n is the total number of nodes) from Segment K and Surface S (of the headform or the respirator), the distance function $Dist(\mathbf{v}_i, S)$ is defined as follows:

- if the projection of i along the z axial direction intersects with Surface S at Point j,

$$Dist(\mathbf{v}_i, S) = \mathbf{v}_j - \mathbf{v}_i, \tag{1}$$

where $\mathbf{v}_i$ is the position vector of point i and $\mathbf{v}_j$ is the position vector of the point j;

- if the projection of i along the z axial direction does not intersect with Surface S,

$$Dist(\mathbf{v}_i, S) = [0,0,0]^T. \tag{2}$$

There are five steps to calculate $Dist(\mathbf{v}_i, S)$.

Step 1: Project Surface S along the z axial direction on the xoy plane to obtain new Surface S', and find Vertex k of S', which has the shortest distance to i among all vertices of S'.

Step 2: Find triangles that share Vertex k. If Point j exists, i should fall in one of these triangles that share Vertex k.

Step 3: Find Triangle T', which contains i and is the projection of the triangle T of Surface S, as shown in Fig. 4. Because the x- and y-coordinates of j are equal to the ones of i, the problem of determining whether j lies inside T equals to determining whether i lies inside T'. Because the coordinates of three vertices of T are known, the positions of T' on the xoy plane can be obtained. We can use the method described by Topping et al. [18] to determine whether a point lies inside a triangle. If three triangles ($\triangle iT_1'T_2'$, $\triangle iT_2'T_3'$, and $\triangle iT_3'T_1'$), constructed by i and any two vertices of T' (in counter clockwise order) are all in counter-clockwise, i lies inside T'. If a triangle $\triangle ABC$ is in the counter clockwise direction,

$$\begin{vmatrix} x_A & y_A & 1 \\ x_B & y_B & 1 \\ x_C & y_C & 1 \end{vmatrix} < 0, \tag{3}$$

where x and y represent the x- and y-coordinates.

Step 4: Calculate $\mathbf{v}_j$ by solving the equation,

$$(\mathbf{v}_j - \mathbf{v}_{T1}) \bullet [(\mathbf{v}_{T1} - \mathbf{v}_{T2}) \times (\mathbf{v}_{T1} - \mathbf{v}_{T3})] = 0, \tag{4}$$

where $\mathbf{v}_{T1}$, $\mathbf{v}_{T2}$, and $\mathbf{v}_{T3}$ are the position vectors of Nodes T_1, T_2, and T_3.

Step 5: Obtain the distance function by applying $\mathbf{v}_j$ to equation (1).

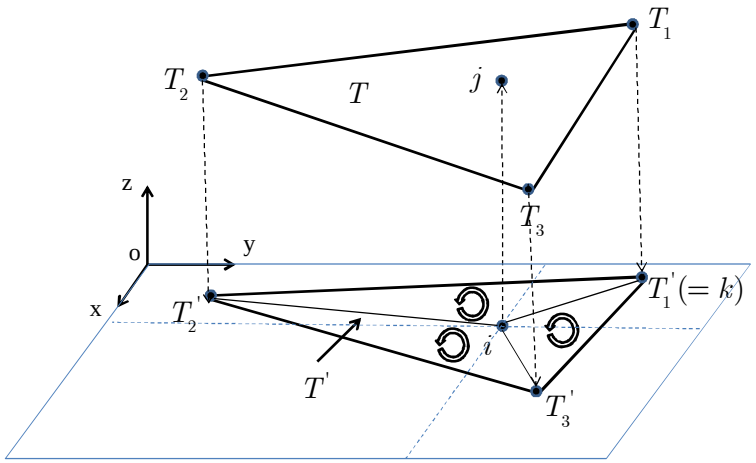

Fig. 4: Node j is the projection of Node i onto Triangle T along the z axial direction, and Triangle T' is the projection of T onto the xoy plane along the -z axial direction.

2.3 Node Distribution

After we have two distance functions $Dist(\mathbf{v}_i, S_1)$ and $Dist(\mathbf{v}_i, S_2)$, where $\mathbf{v}_i$ ($i = 1,2,3,...,n$, where n is the total number of nodes) is the position of Node i on Segment K and S_1, S_2 are the surfaces of the headform and respirator, respectively, new nodes are distributed in the interior of the volume bounded by two surfaces. For Node i on Segment K with a position vector $\mathbf{v}_i$, we calculate two distance function values $\mathbf{D}_1$ ($= Dist(\mathbf{v}_i, S_1)$) and $\mathbf{D}_2$ ($= Dist(\mathbf{v}_i, S_2)$) with respect to Surfaces S_1 and S_2. If the distance function value $\mathbf{D}_1$ (or $\mathbf{D}_2$) equals to zero, Node i cannot be projected to Surface S_1 (or S_2) and it can be ignored in further processing. If $\mathbf{D}_1$ equals to $\mathbf{D}_2$, two surfaces contact at the location with the same x-, y-coordinates of Node i and Node i can also be ignored in this circumstance. To-be-meshed volume exits for Node i only if $\mathbf{D}_1$ is less than $\mathbf{D}_2$, and they are collected as potential nodes.

For Node i that is one of the potential nodes, new Nodes N_i^k (k=1,2,3,**é**,m, where m is the total number of new nodes generated by Node i) are inserted in the line that is constructed by linking points ($\mathbf{v}_i + \mathbf{D}_1$) and ($\mathbf{v}_i + \mathbf{D}_2$). All these new nodes have the same x-, y-coordinates of Node i. There are two ways to distribute nodes along z axial direction. One uses a uniform number of nodes and the other uses a uniform spacing size. In the first method, every potential node generates the same number of new nodes. The z-coordinates of Nodes N_i^k (k=1,3,4**é**,m) equal to $\mathbf{v}^{z-}{}_i + (k-1)\times(\mathbf{D}_2 - \mathbf{D}_1)$, where $\mathbf{v}^{z-}{}_i$ is the z-coordinate of Node i. In the second method, a mesh size along the z axial direction can be predefined, for example, as 1 mm, for all elements besides the ones on the boundary. The z-coordinates of Nodes N_i^1 and N_i^m are $\mathbf{D}_1$ and $\mathbf{D}_2$, so that N_i^1 and N_i^m are placed on Surface S_1 and S_2. The z-coordinates of Nodes N_i^k (k=2,3,4**é**,m-1) are uniformly spaced between ($\mathbf{v}^{z-}{}_i + \mathbf{D}_1$) and ($\mathbf{v}^{z-}{}_i + \mathbf{D}_2$) with spacing size 1 mm and integer number values. Because the headform and respirator surfaces are closed to each other or, even, contact, the meshed volume has very complicated geometrical features and the uniform number method should be used.

2.4 Volume Pentahedralization

After distribution of new nodes, methods for generating volumetric elements are investigated. The most straightforward method is Delaunay triangulation, since MATLAB software has a function to directly generate Delaunay triangulation using the position vectors of a set of points. However, since Delaunay method creates a convex mesh and the volume between two surfaces is not always convex, an additional process of boundary recovery is necessary. Other than Delaunay triangulation, this paper achieves a 3D pentahedral mesh generation in the volume by the method of decomposing pseudo hexahedral elements. First, we select a starting surface (for example the headform surface) and nodes on this surface are chosen as the starting nodes. Second, each starting node searches its neighboring nodes in the z and approximately x, y axial direction. Third, by connecting every set of eight neighboring nodes, pseudo hexahedral elements are constructed. These elements are not real hexahedra, because each face of a real hexahedron should have four vertices, which can construct a plane, and a pseudo hexahedral may have four vertices in one of its face that are able to construct a plane. Fourth, each pseudo hexahedron is divided into two pentahedral elements. As shown in Fig. 5, a hexahedron ($\overline{ABCDEFGH}$) is used to create two pentahedrons ($\overline{ABCDFG}$ and $\overline{ADEFGH}$). The advantage of pentahedral mesh is that nodes can move along z axial direction without damaging the elemental structure. The first layer of pentahedral elements is generated between the headform and respirator surfaces. The surface of the first layer on the side that is opposite the headform surface is set as the new surface and a new layer of pentahedrons is produced by repeating the procedures described above. Finally, element layers fully occupy the volume between two inputting surfaces.

2.5 Element Smooth

A geometrical fairing technique, so called signal processing method, is used for smoothing the volumetric mesh [16],[17]. First, for every node in the pentahedral mesh its neighboring nodes are set as the signals and their indices are recorded. Although node n may have more than six neighbor nodes, only the ones in the z and -z axial directions and in the approximately x, -x, y and -y axial directions are selected. The set of neighboring nodes of Node n are denoted by n^*. Second, using the method developed by Boyd and Müller [3], all nodes are classified into three types (fixed nodes, surface nodes and interior nodes) and their recorded neighbors are adjusted according to their types. The interior nodes are defined as the nodes with six neighboring nodes and their neighborhood records are not changed in this step. The fixed nodes are defined as the nodes with whose positions are fixed during the smoothing process. Then, the records of all neighboring nodes of the fixed nodes are deleted, so that they are not influenced by their signals. The surface nodes are defined as the nodes located on the surface of the volume and have five or six neighbors. Then, among their neighbors the records of interior nodes are deleted, so that the surface nodes are only influenced by the signals of the neighbors in the types of fixed nodes and surfaces nodes. Third, a discrete Laplacian is defined for each node according to the equation:

$$\Delta \mathbf{v}_n = \sum_{m \in n^*} w_{nm} (\mathbf{v}_m - \mathbf{v}_n) , \tag{5}$$

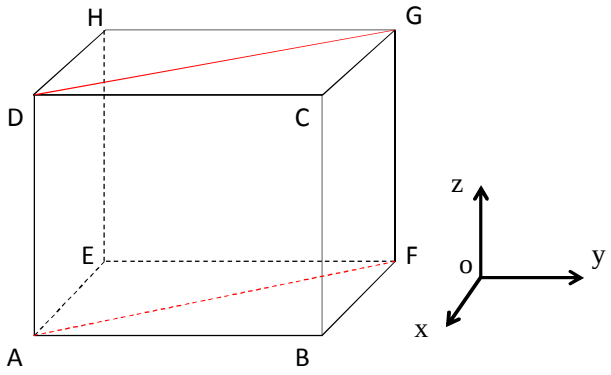

Fig. 5: Decomposition of a hexahedral element into two pentahedral elements.

where w_{nm} are the weights for all neighbors. Since the distribution of nodes is approximately uniform, we use a simplest way to obtain the weights, $w_{nm} = 1/k$, where k is the total number of neighbor nodes for node n [16]. Forth, we conduct smoothing iterations. Every iteration has a shrinking step and an un-shrinking step that are mathematically expressed as

$$\mathbf{v}_n^{new} = \mathbf{v}_n^{old} + \lambda \Delta \mathbf{v}_n^{old} \tag{6}$$

$$\mathbf{v}_n^{new} = \mathbf{v}_n^{old} + \mu \Delta \mathbf{v}_n^{old} \tag{7}$$

where λ and μ are two scaling factors and $0 < \lambda < 1$, $-1 < \mu < -\lambda$.

Boyd and Müller [3] and Flaig [6] applied the signal processing method to the hexahedral mesh. However the constraints of nodal displacements were not discussed in their papers. For a hexahedral element with eight vertices and six faces, its nodes cannot arbitrarily displace, because one of its faces may have four nodes that are not on the same plane after nodal displacements. This paper applies the signal processing method to the pentahedral mesh. In Fig. 5, a pentahedron $\overline{ABCDFG}$ has six nodes and five faces. Edges $\overline{AD}$, $\overline{BC}$ and $\overline{FG}$ should always be perpendicular to the xoy plane in order to make sure each of faces $\overline{ABCD}$, $\overline{BCFG}$ and $\overline{ADFG}$ on a plane. Faces $\overline{ABF}$ and $\overline{CDG}$ are triangles that are always on planes. Thus, nodes can only move in the z axial direction and their movements in the x, y axial direction are constrained. During iterations, the edge lengths are checked. If a node has an edge whose length is shorter than a tolerance, its position is fixed. Fig. 6 presents an example for the element smooth method.

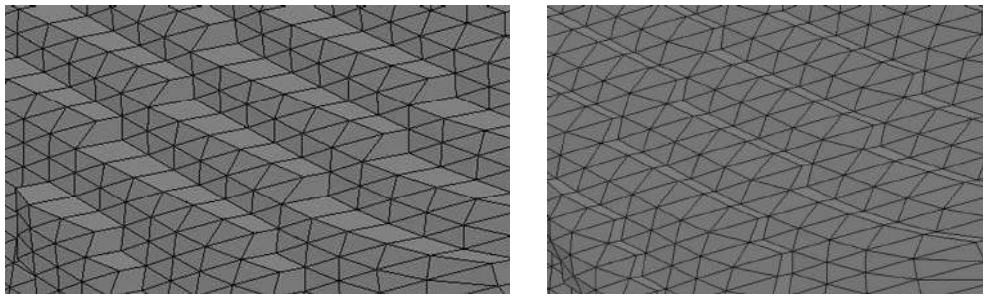

(a) (b)

Fig. 6: the surface of a pentahedral mesh having sharp edges (a) before element smooth; (b) after element smooth.

2.6 Virtual Surface

We consider the problem of meshing the volume defined by a surface and a list of control points. A facial surface extracted from a medium size headform is used [28]. De Greef et al. [7] showed a database of Caucasian facial soft tissue thickness using a large-scale in-vivo study. According to this database, we define 14 points of the facial surface that have predetermined values of depths, as shown in Fig. 7. In order to cover the entire surface, 4 points with 0 values of depths are also added. The objective is to generate a volumetric mesh for the facial soft tissue layer that has different thicknesses at these predefined 14 points.

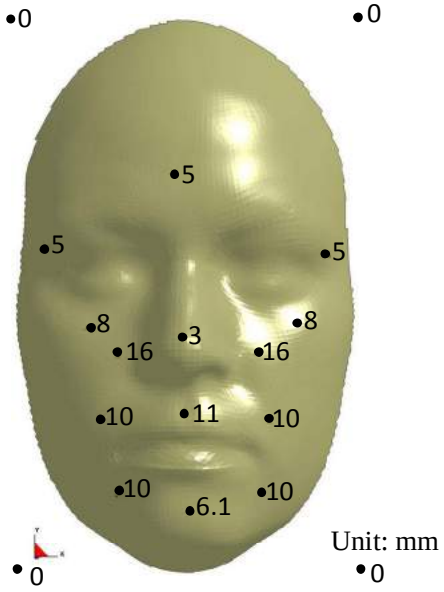

Fig. 7: A facial surface with predetermined depths at 18 locations.

The inputs are the facial surface and 18 control points. Similar to the method described in previous section, the facial surface S_1 is placed in the Cartesian coordinate system where the coordinate system xoy is similarly defined as Section 2. Using these 18 control points, we create a set of new points whose x-, y- coordinates are as the same as these 18 control points, and whose z-coordinates equal to the predefined tissue thicknesses. Then, a virtual surface S_2 that contains these 18 new points is generated using Delaunay triangulation, as shown in Fig. 8.

The facial surface and the virtual surface are both projected onto the xoy plane. Similarly, we find Segment K that contains the union of the projecting areas of two surfaces. For Node i on Segment K, applying its position vector $\mathbf{v}_i$ and the facial surface S_1 and the virtual surface S_2 to distance functions, we obtain two values $\mathbf{D}_1$ $(= Dist(\mathbf{v}_i, S_1))$ and $\mathbf{D}_2$ $(= Dist(\mathbf{v}_i, S_2))$ with respect to surfaces S_1 and S_2. New nodes N_i^k (k=1,2,3,…,m, where m is the total number of new nodes generated by node i) are inserted in the line that links points $(\mathbf{v}_i + \mathbf{D}_1)$ and $(\mathbf{v}_i + \mathbf{D}_1 - \mathbf{D}_2)$. The nodes N_i^k (k=2, 3, 4…, m-1) are distributed with a uniform spacing 1 mm, while N_i^1 and N_i^m are in the position of $(\mathbf{v}_i + \mathbf{D}_1)$ and $(\mathbf{v}_i + \mathbf{D}_1 - \mathbf{D}_2)$. The procedures of generating pentahedrons and smoothing the volumetric mesh are similar to the procedures in the two surfaces problem.

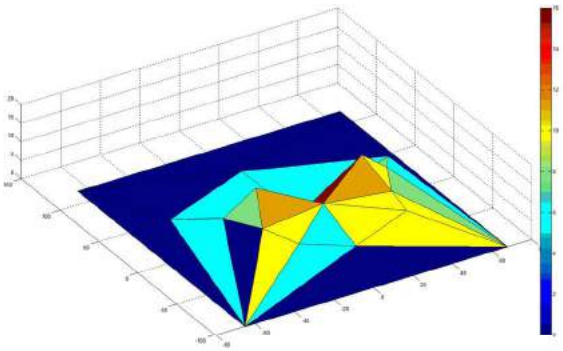

Fig. 8: A virtual surface based on 18 control points.

3 APPLICATIONS

This section provides two applications, CFD simulation of air leakage of headform/respirator and finite element contact simulation of headform/respirator, that use our proposed method for mesh generation. We developed two MATLAB-based algorithms for solving two different problems described in the introduction section, namely pentahedral mesh of a volume bounded by two surfaces and pentahedral mesh of a volume defined by a surface and a list of control points. All mesh generations are performed at a regular PC workstation equipped with an Intel(R) Core(TM)2 Duo CPU 2.14GHz and a 4.00 GB memory.

The first application is to solve a coupled effort of the air flow and the heat convection around the face of the headform for detecting the leakage of headform/respirator using CFD method. The air flow field includes three zones: between the headform and the respirator, inside the respirator medium and outside of the respirator. Since the method of meshing the volume between two surfaces has been investigated, we defined four surface-pairs, including headform/respirator inner, respirator inner/respirator outer, respirator outer/exterior and headform/exterior, and the volume between each surface-pair was meshed. The dimension of the whole meshed domain in z axial direction was 160 mm. Zone I consisted of five layers of elements, which had the same thickness at the arbitrary location with the same x and y coordinate. Zone II had one layer of elements with a uniform thickness of 3 mm that was the thickness of respirator filtering medium. Zone III had a structure of twenty-six layers with 6 boundary layers and a structure of twenty layers without 6 boundary layers. The 6 boundary layers had the thickness of 0.5 mm and other layers in Zone III had the thickness of 7.7 mm. The dimensions and mesh element sizes in the x and y axial directions were controlled by Segment K in the xoy plane. We chose Segment K as a rectangular with a width of 232 mm in the x axial direction and a height of 251 in the y mm axial direction. In the middle area of Segment K where the nodes could be projected on the respirator surface along the z axial direction the mesh element size is 2 mm, while in other area of Segment K the mesh element size is 5 mm. Fig. 9 shows the volumetric mesh of Zone I-III, having totally 201318 nodes and 378400 pentahedral elements. The computation CPU time, which included the processes of reading the data, generating distance functions, creating nodes and elements, and smoothing the mesh, was 161.22 seconds. ANSYS FLUENT software was adopted to check the quality of the volumetric mesh. Maximum cell squish was 0.975, maximum cell skewness was 0.945 and maximum aspect ratio was 342. All three indices passed the quality criteria in ANSYS FLUENT. Thus, our proposed method provided this CFD application a volumetric mesh with acceptable mesh quality, although the quality was not perfect. Fig. 10 presents the simulation result of the evolution of the temperature contour in the first breathing cycle.

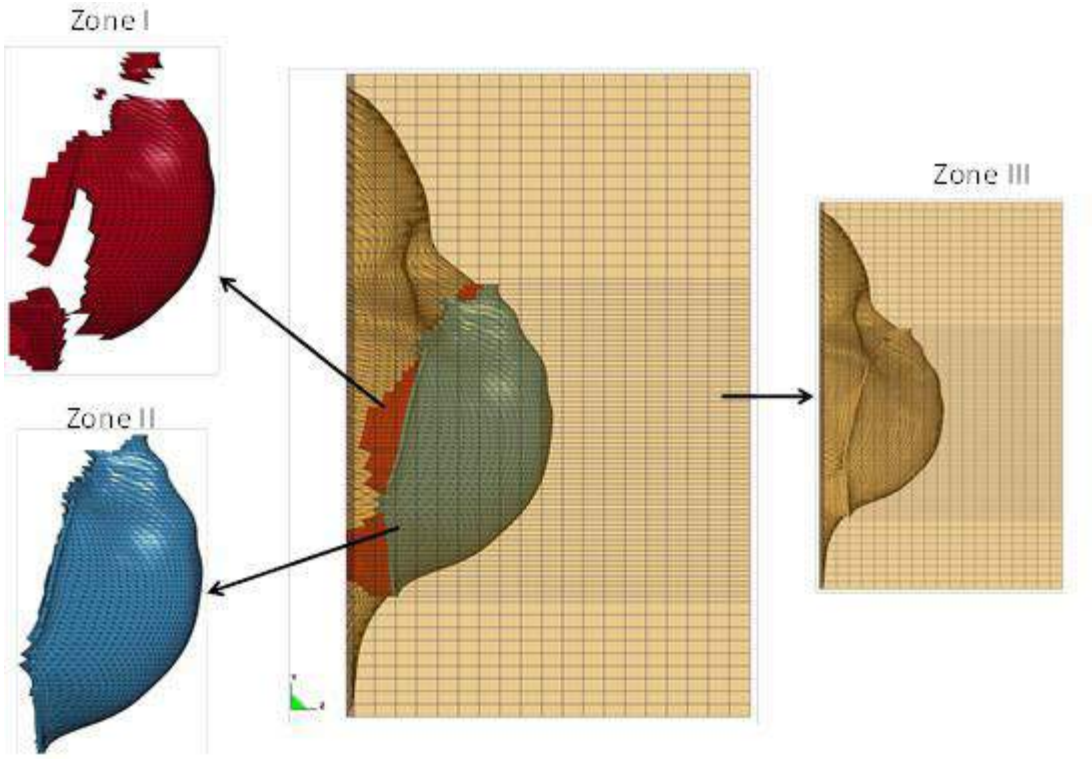

Fig. 9: Mesh generation in zone I (the volume between the headform and the inner surface of the respirator), zone II (inside the respirator's medium) and zone III (outside of the respirator).

The second application is to simulate the contact between a headform and a respirator. Our proposed method was used in meshing a human facial model that had predetermined soft tissue thicknesses at different sites. Fig. 11(a) shows the finite element model of human face consisting of 20992 nodes and 29164 pentahedral elements. Fig. 11 (b) presents the model's interface that was cut by the zoy plane. The soft tissue thicknesses at different facial sites indicated a high bio-fidelity. It took CPU time 58.69 seconds to create volumetric mesh. ANSYS FLUENT software was also used to exam the quality of the volumetric mesh. Maximum cell squish was 0.803, maximum cell skewness was 0.855 and maximum aspect ratio was 38. The mesh quality in this application is better than the one in the first application. Fig. 12(a) presents the final stage of the contact simulation in which the respirator contacted the human face. Fig. 12(b) shows the contact pressure distribution on the human face, which is essential to respirator fit and comfort.

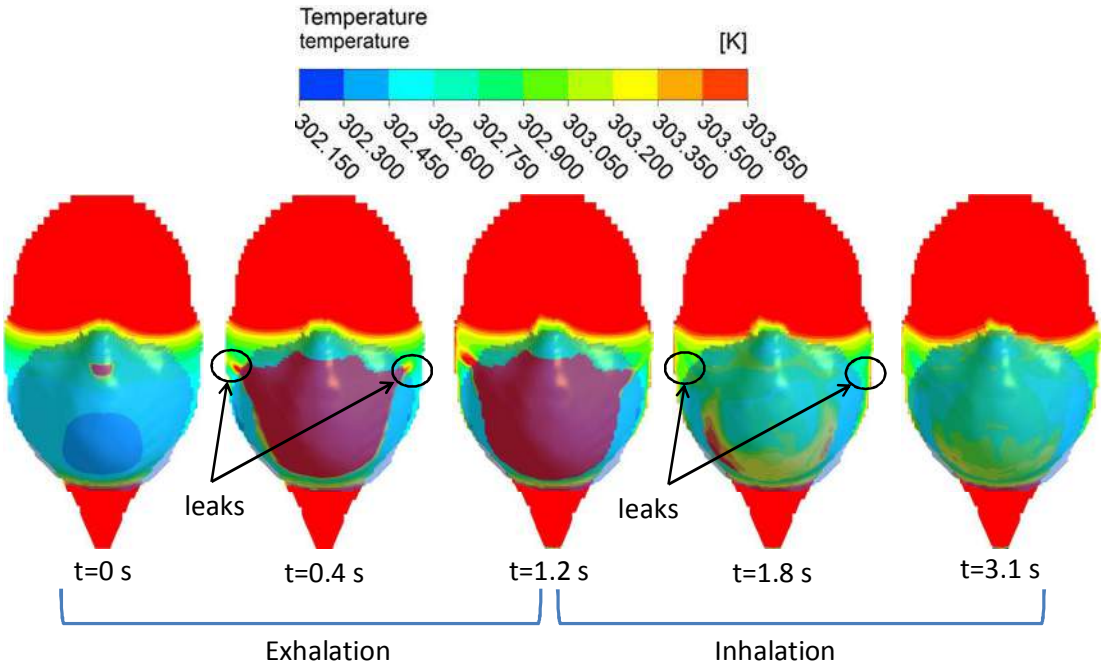

Fig. 10: The temperature contours in the first breathing cycle.

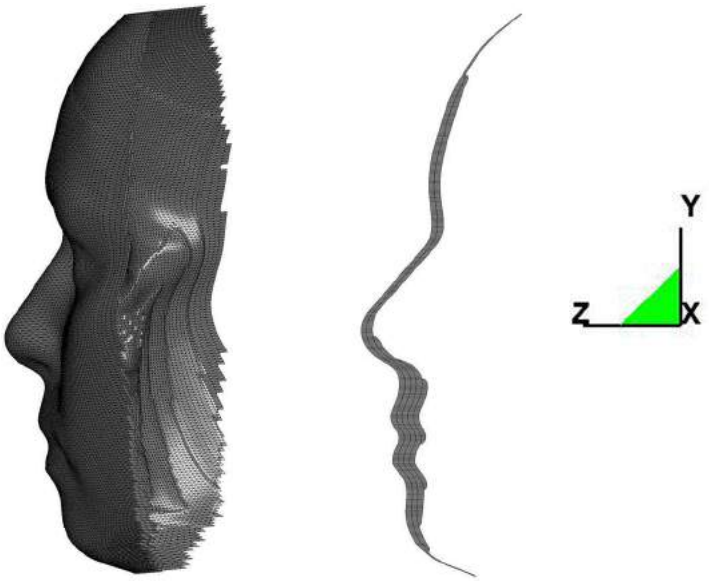

(a) (b)

Fig. 11: Finite element model of human face that has predefined soft tissue thicknesses at different sites, (a) the whole face model; (b) the interface cut by the z-y plane.

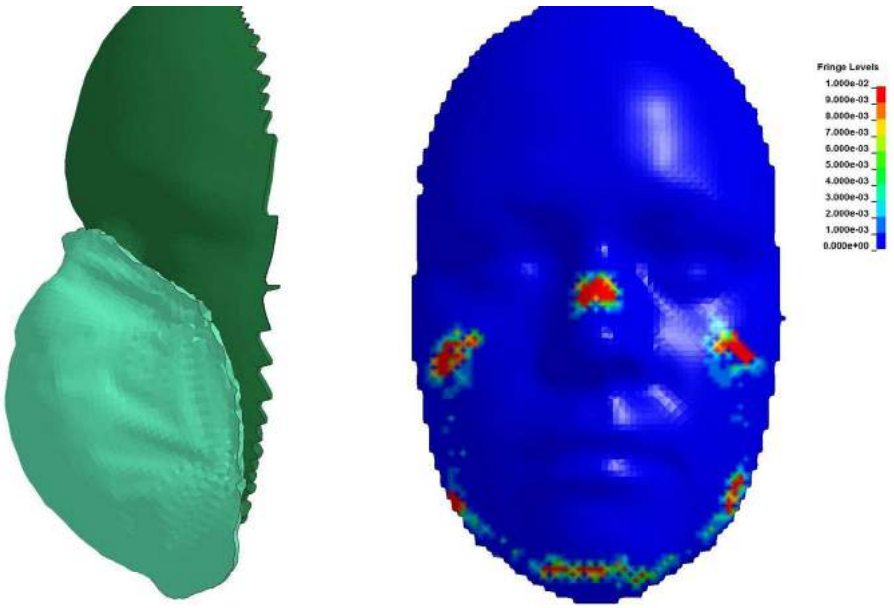

(a) (b)

Fig. 12: (a) The respirator contacts the human face; (b) the contact pressure distribution on the human face (MPa).

4 CONCLUSION AND FUTURE WORK

This paper provided innovative algorithms on generating layered pentahedral mesh using unclosed surfaces and nodes (a volume bounded by two surfaces or a surfaces and a list of control points). Illustration examples for meshing the deadspace of a respirator and a finite element model of human face were demonstrated for these two cases. We defined the distance function that described the relative distance between a surface and a plane. Using two distance functions, a volume with a complicated geometrical feature can be described mathematically. Pentahedral elements were generated by decomposing pseudo hexahedral elements, and the volumetric mesh is achieved by adding layers of pentahedral elements. A signal processing method was adopted for smoothing the volumetric mesh. Our proposed methods were adopted in two applications, CFD simulation of air leakage of headform/respirator and finite element simulation of contact between a headform and respirator. Results of two applications indicate that our automatic mesh generation algorithms are a useful tool for biomechanical simulations that contain highly curved geometries in which obtaining a closed surface for volumetric mesh is extremely difficult.

Using our mesh generation methods, generating distance functions dominates the CPU time. Future study will focus on optimizing the algorithm of producing distance functions. Since the MATLAB implement is usually slow, a C++ or FORTRAN version of the program is in need in order to shorten the calculation time. Although the mesh quality in the applications was acceptable, a method to increase the mesh quality needs to be investigated.

REFERENCES

[1] Anthony T. R.; Flynn M. R.: Computational fluid dynamics investigation of particle inhalability, Journal of Aerosol Science, 37, 2006, 750-765. http://dx.doi.org/10.1016/j.jaerosci.2005.06.009

[2] Barbarino, G. G.; Jabareen, M.; Trzewik, J.; Nkengne, A.; Stamatas, G.; Mazza, E.: Development and validation of a three-dimensional finite element model of the face, Journal of Biomechanical Engineering, Volume 131, Issue 4, 2009. http://dx.doi.org/10.1115/1.3049857.

[3] Boyd, S.K.; Müller, R.: Smooth surface meshing for automated finite element model generation from 3D image data, Journal of Biomechanics, 39, 2006, 1287-1295. http://dx.doi.org/10.1016/j.jbiomech.2005.03.006 PMid:15922348

[4] Chan, C.; Anastasiou, K.: An automatic tetrahedral mesh generation scheme by the advancing front method, Communications in Numerical Methods in Engineering, 13, 1997, 33-46. http://dx.doi.org/10.1002/(SICI)1099-0887(199701)13:1<33::AID-CNM39>3.0.CO;2-R

[5] Craven B. A.; Settles G. S.: A computational and experimental investigation of the human thermal plume, Journal of Fluid Engineering, Volume 128, November, 2006.

[6] Flaig, P.A.C.: On smoothing surfaces in voxel based finite element analysis of trabecular bone, Large-scale scientific computing: 6th international conference, LSSC 2007, Sozopol, Bulgaria, June 5-9, 2007: revised papers, 4818, p.69.

[7] De Greef, S. et al.: Large-scale in-vivo Caucasian facial soft tissue thickness database for craniofacial reconstruction, Forensic science international, 159, 2006, 126-S146. http://dx.doi.org/10.1016/j.forsciint.2006.02.034 PMid:16563680

[8] Ito, Y., Shih; A.M.; Soni, B.K.: Octree-based reasonable-quality hexahedral mesh generation using a new set of refinement templates, International Journal for Numerical Methods in Engineering, 77, 2009, 1809-1833. http://dx.doi.org/10.1002/nme.2470

[9] Lee, C. Y.; Lee, S.; Chin, S.: Multi-layer structural wound synthesis on 3D face. Computer Animation and Virtual Worlds, Volume 22, Issue 2-3, 2011, 117-185.

[10] Lei, Z.; Yang, J.: Methodology for simulating air leakages of an N95 filtering facepiece respirator-a pilot study, Computer-Aided Design and Applications, Vol. 9, Issue 1, 2012, 43-53.

[11] Lei, Z.; Yang, J.; Zhuang, Z.: Headform and N95 filtering facepiece respirator interaction: contact pressure simulation and validation, Journal of Occupational and Environmental Hygiene, 9, 2012, 46-58. http://dx.doi.org/10.1080/15459624.2011.635130 PMid:22168255

[12] Li Y.; Li F.; Zhu Q.: Numerical simulation of virus diffusion in facemask during breathing cycles, International Journal of Heat and Mass Transfer, 48, 2005.

[13] Keeve, E.; Girod, S.; Kikinis, R.; Girod, B.: Deformable modeling of facial tissue for craniofacial surgery simulation. Computer Aided Surgery, Volume 3, No. 5, 1998, 228-238 http://dx.doi.org/10.3109/10929089809149844 PMid:10207647

[14] Mao A.; Li Y.: Numerical heat transfer coupled with multidimensional liquid moisture diffusion in porous textiles with a measureable-parameterized model, Numerical Heat Transfer, Part A, 56, 2009, 246-268. http://dx.doi.org/10.1080/10407780903163330

[15] Shewchuk, J.R.: Delaunay refinement algorithms for triangular mesh generation, Computational Geometry, 22, 2002, 21-74. http://dx.doi.org/10.1016/S0925-7721(01)00047-5

[16] Taubin, G.: A signal processing approach to fair surface design, Proceedings of the 22nd annual conference on Computer Graphics and Interactive Techniques, 1995, 351-358.

[17] Taubin, G.: Geometric signal processing on polygonal mesh, Eurographics, 2000.

[18] Topping, B.H.V., Muylle, J., Ivanyi, P., Putanowicz, R. and Cheng, B.: Finite element mesh generation, Saxe-Coburg Publications, Stirling, UK, 2004.

[19] Waters, K.: Physical model of facial tissue and muscle articulation derived from computer tomography data, Surgery and Treatment Planning, Volume 1808, 574, 1992.

[20] Zhang, Y.; Bajaj, C.: Adaptive and quality quadrilateral/hexahedral meshing from volumetric data, Computer Methods in Applied Mechanics and Engineering, 195, 2006, 942-960. http://dx.doi.org/10.1016/j.cma.2005.02.016 PMid:19750180 PMCid:2740490

[21] Zhang, Y.; Bajaj, C.; Sohn, B.S.: 3D finite element meshing from imaging data, Computer Methods in Applied Mechanics and Engineering, 194, 2005a, 5083-5106. http://dx.doi.org/10.1016/j.cma.2004.11.026 PMid:19777144 PMCid:2748876

[22] Zhang, Y.; Bajaj, C.; Xu, G.: Surface smoothing and quality improvement of quadrilateral/hexahedral mesh with geometric flow, Proceedings of the 14th International Meshing Roundtable, 2005b, 449-468. http://dx.doi.org/10.1007/3-540-29090-7_27

[23] Zhang, Y.; Hughes, T.J.R.; Bajaj, C.L.: An automatic 3D mesh generation method for domains with multiple materials, Computer Methods in Applied Mechanics and Engineering, 199, 2010, 405-415. http://dx.doi.org/10.1016/j.cma.2009.06.007 PMid:20161555 PMCid:2805160

[24] Zhang, Y.; Sim, T.; Tan, C. L.; Sung, E.: Anatomy-based face reconstruction for animation using multi-layer deformation, Journal of Visual Languages and Computing, Volume 17, Issue 2, 2006, 126-160. http://dx.doi.org/10.1016/j.jvlc.2005.10.002

[25] Zhuang, Z.; Bradtmiller, B.: Head-and-face anthropometric survey of US respirator users, Journal of Occupational and Environmental Hygiene, 2, 2005, 567-576. http://dx.doi.org/10.1080/15459620500324727 PMid:16223715

[26] Zhuang, Z.; Benson, S.; Viscusi, D.: Digital 3-D headforms with facial features representative of the current US workforce, Ergonomics, 53, 2010, 661-671. http://dx.doi.org/10.1080/00140130903581656 PMid:20432086

[27] Zhuang, Z.; Bradtmiller, B.; Shaffer, R.E.: New respirator fit test panels representing the current US civilian work force, Journal of Occupational and Environmental Hygiene, 4, 2007, 647-659. http://dx.doi.org/10.1080/15459620701497538 PMid:17613722

[28] Zhuang, Z.; Slice, D.E.; Benson, S.; Lynch, S.; Viscusi, D.: Shape analysis of 3D head scan data for US respirator users, EURASIP Journal on Advances in Signal Processing, 2010, 2-2.